Journal of Archaeological Science 36 (2009) 461–466

Contents lists available at ScienceDirect

Journal of Archaeological Science

journal homepage: http://www.elsevier.com/locate/jas

Trace element fingerprinting of ancient Chinese gold with femtosecond laser ablation-inductively coupled mass spectrometry

Lynn B. Brostoff [a,*], Jhanis J. González [b], Paul Jett [c], Richard E. Russo [b]

[a] Library of Congress, Preservation Research and Testing Division, 101 Independence Avenue, SE, Washington, DC 20540, USA
[b] Lawrence Berkeley National Laboratory, 1 Cyclotron Road, Berkeley, CA 94720, USA
[c] The Freer Gallery of Art/Arthur M. Sackler Museum, Smithsonian Institution, Washington, DC 20013, USA

ARTICLE INFO

Article history:
Received 8 May 2008
Received in revised form
22 September 2008
Accepted 22 September 2008

Keywords:
Femtosecond
LA-ICP-MS
Trace element
Ancient gold

ABSTRACT

In this collaborative investigation, femtosecond laser ablation-inductively coupled mass spectrometry (LA-ICP-MS) was applied to the study of a remarkable group of ancient Chinese gold objects in the Smithsonian's Freer Gallery of Art and Arthur M. Sackler Gallery. Taking advantage of the superior ablation characteristics and high precision of a femtosecond 266 nm Ti:sapphire laser at Lawrence Berkeley National Laboratory, major, minor and trace element concentrations in the gold fragments were quantified. Results validate use of femtosecond LA-ICP-MS for revealing "fingerprints" in minute gold samples. These fingerprints allow us to establish patterns based on the association of silver, palladium and platinum that support historical, technical and stylistic relationships, and shed new light on these ancient objects.

1. Introduction

This investigation describes femtosecond laser ablation-inductively coupled mass spectrometry (fs-LA-ICP-MS) analysis of a group of exquisite gold foil fragments from the collection of the late Dr Paul Singer in the Smithsonian's Freer Gallery of Art and Arthur M. Sackler Gallery (Fig. 1). The objects are thought to originate from the late Eastern Zhou period in China, ca. 5–6th century BCE. Originally, the fragments, which range in size from 1 × 1 cm to 18 × 13 cm, were attached to bronze supports and may have been produced as coffin decoration. However, the exact function of the pieces, their method of manufacture, and their relationship to one another, have long been a mystery. Therefore, the Freer Gallery, in collaboration with the Smithsonian's Museum Conservation Institute (MCI), undertook an in-depth technical study of these interesting and well-known pieces (Jett et al., 2007). The study also investigated the relationship of the Singer fragments to other ancient Chinese gold foil decorated objects in the museum's collection, including a gold-decorated bronze disk shown in Fig. 2. Although the latter object has been attributed to a different archaeological site than the Singer fragments[1], stylistic and technical characteristics are strikingly similar, as revealed in the superimposed drawing of the object's detailed surface decoration.

Prior to any detailed elemental analysis, X-ray fluorescence spectroscopy (XRF) conducted at the Freer Gallery revealed that the objects have similar overall compositions, with 92–94% gold and no other appreciable major constituents except silver (Jett et al., 2007). Careful technical examination of the Singer fragments also revealed that the foil was hammered, and that the low-relief decoration was produced by inscribing intricate patterns of writhing and interlacing snakes or dragons on both sides of the sheets (Fig. 3a). Although only three fragments were found to join together, a virtual reconstruction based on overlapping fragments convincingly revealed that eight of the Singer fragments are from six separate plaques, the original form of which may have been a writhing dragon; three of the plaques would have faced left and three have faced right. The proposed reconstruction of a plaque is shown in Fig. 3b. The surface decoration on the fragments would thus have echoed the final form of the plaque. Six additional fragments are most likely from dragon plaques, and the remaining objects appear to be from other types of plaques that are known from this period (Jett et al., 2007).

Although it is possible to work gold directly, without prior refining, alloying of the metal will improve its working properties and its overall aesthetic appearance. Both the consistency of the silver content in the Singer fragments, and the physical form of the foil, including its uniformity of thickness (about 10–50 μm), suggest that the gold was processed in a fairly controlled manner. These

* Corresponding author. Tel.: +1 301 238 1211; fax: +1 301 238 2709.
E-mail addresses: lbrostoff@loc.gov, lbb323@yahoo.com (L.B. Brostoff).

[1] Most scholars believe the Singer fragments are from one site, although its location remains uncertain. The bronze disc has been attributed to a different, but also uncertain site.

0305-4403/$ – see front matter © 2008 Published by Elsevier Ltd.
doi:10.1016/j.jas.2008.09.037

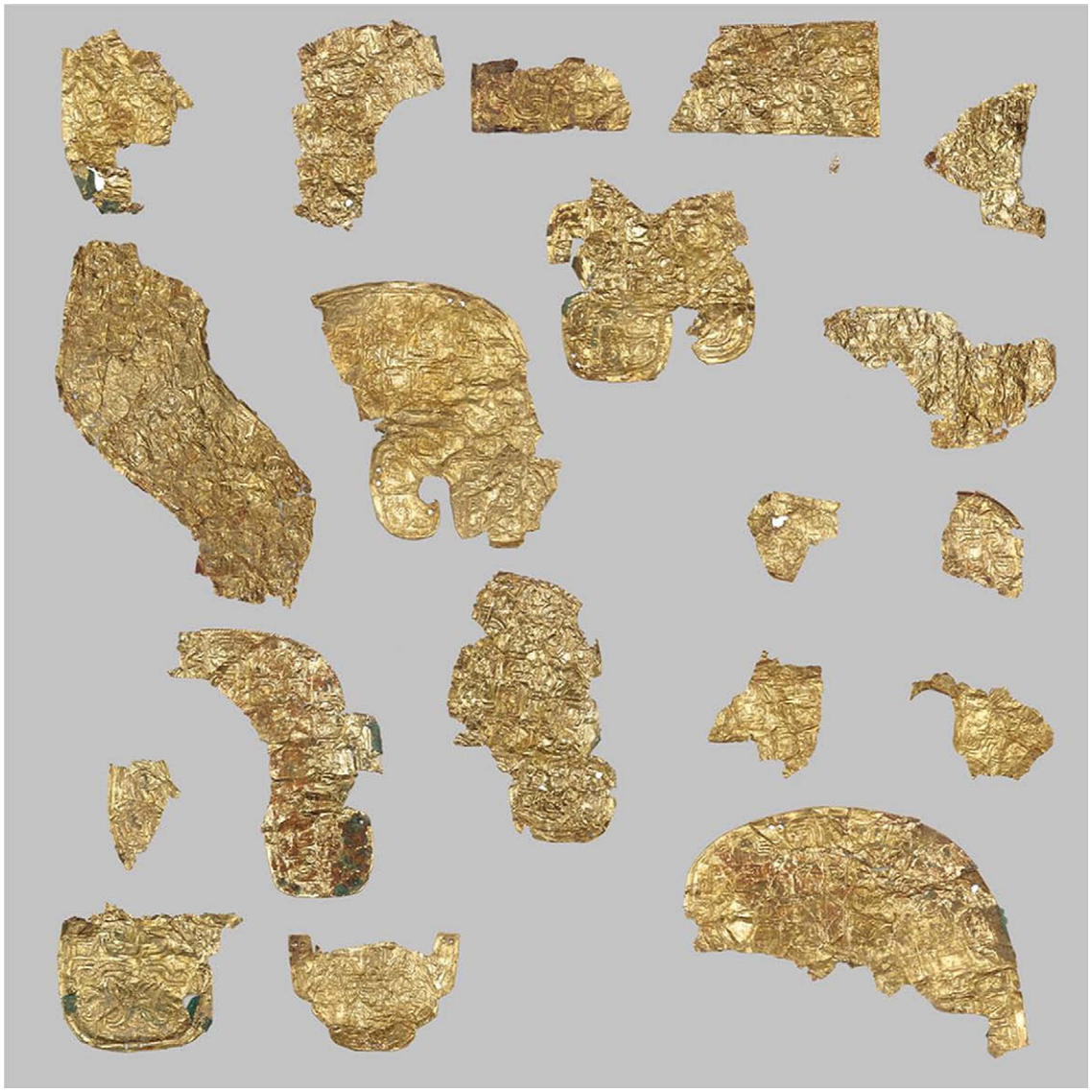

Fig. 1. Twenty-one fragments of ancient Chinese decorative gold foil fragments (1 × 1 cm to 18 × 13 cm), Eastern Zhou period, ca. 6th century BCE, in the collection the Freer Gallery of Art and Arthur M. Sackler Gallery, Smithsonian Institution. (With permission of Freer Gallery of Art and Arthur M. Sackler Gallery, Smithsonian Institution; figures also published in Jett et al., 2007.)

objects thus represent a high level of craftsmanship and technological achievement. In particular, they coincide with a sudden flourishing of gold finds dating from about the 5–6th century BCE, which may relate to an advance in metallurgical skills or production, or to a growing interest in "exotic objects" (von Falkenhausen, 2006). Therefore, the relationship of these precious objects to ancient gold sources and/or craft workshops is of great historical and technical import.

Fig. 2. Gold foil decorated bronze disc (13 cm diameter), 4506, with overlaid drawing of surface decoration. (With permission of Freer Gallery of Art and Arthur M. Sackler Gallery, Smithsonian Institution.)

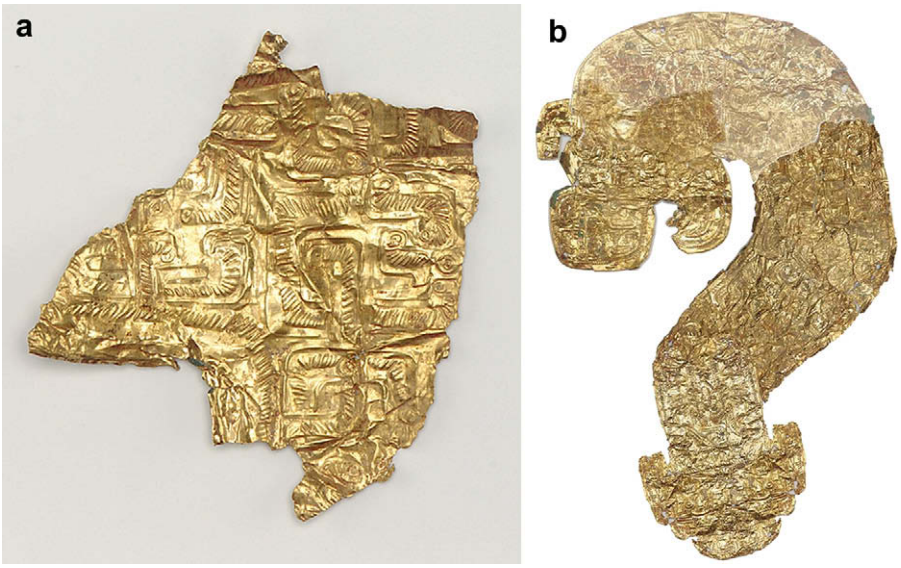

Fig. 3. (a) Close-up of Singer fragment 4504 Q (6 × 6 cm), and (b) hypothetical reconstruction of dragon plaque (27 × 17 cm) based on Singer fragments. (With permission of Freer Gallery of Art and Arthur M. Sackler Gallery, Smithsonian Institution; figures also published in Jett et al., 2007.)

Although significant variation in composition may exist within a placer gold deposit, patterns of inter-element associations, or "fingerprints," may exist for a large number of objects manufactured from the same gold ore (Leake et al., 1993; Watling et al., 1994; Watling et al., 1999; Ixer, 1999; Guerra, 2004b; Guerra et al., 2005). Among elements that may be geologically associated with gold ore, platinum group elements, including palladium, platinum, osmium, ruthenium, rhodium and iridium, are of particular interest. Iridium, osmium and ruthenium are most often present as inclusions, which are occasionally visible under magnification. In contrast, trace amounts of palladium (Pd) and platinum (Pt) tend to be homogeneously distributed in gold; these elements also have high melting and boiling point temperatures, so that they should be unaffected by the relatively low temperatures achieved in ancient gold refining and working techniques (Craddock, 1995; Ramage and Craddock, 2000). Based on these assumptions, previous researchers have maintained that trace concentrations of platinum and/or palladium, and their ratio, remain characteristic of the source gold in artifacts (Gondonneau et al., 1996; Hall et al., 1998; Guerra et al., 1999; Watling et al., 1999; Guerra, 2004a,b,c; Guerra et al., 2005).

Actual sourcing or provenancing of gold in relation to manufactured art objects remains problematic, however, due to lack of an extensive database of elemental profiles in gold ores, natural variation in ore geology, and difficulties with accurate analysis of trace elements (Jones, 1983; Guerra et al., 1999; Ixer, 1999; Watling et al., 1999; Guerra, 2004a,c). Moreover, the inevitable trading, looting and re-melting of precious metal objects makes such a task difficult, if not impossible. On the other hand, correlation of Pd and Pt content, along with a detailed elemental analysis, may provide a fingerprint closer to the craftsman himself, i.e. the raw batches of gold or gold alloy used to fashion objects within related workshops. Thus, elemental fingerprinting should be a viable means for internal comparison of groups of objects.

Due to the valuable nature of gold objects, especially in the case of museum objects, sampling may be impossible or at the very least be minimally invasive. Fortunately, in the case of the gold objects from the Freer Gallery, the thinly worked gold has crimped edges that were originally folded over bronze plaques, so that tiny samples, on the order of about 150 × 900 μm, were possible to remove from folded edges. The amount of sample available for analysis, as is typical with gold objects, thus presents a challenge for conventional trace element analytical techniques, including liquid-based ICP-MS, in which amounts of the solid sample in the micrograms range are necessary to produce reliable sample solutions. Laser ablation, however, allows direct sample introduction in sufficient amount to measure trace elements of interest with reasonable precision (Russo et al., 2002; Gunther and Hattendorf, 2005).

In addition to being thin, the Freer Gallery gold samples have rough, uneven surfaces. These conditions present a challenge for laser ablation in terms of finding a method that will not penetrate through the foil samples, yet will optimize the signal output and precision without causing undue fractionation. Fs-LA-ICP-MS offers the unique characteristic of direct multi elemental solid sample characterization using only femtograms of sample, as well as improved ablation characteristics compared to more common nanosecond (ns) LA-ICP-MS, as previously conducted at MCI (Jett et al., 2007; Brostoff et al., 2007). This superiority consists largely in a substantial reduction in heat diffusion throughout the sample, which consequently avoids intense melting, material redistribution, and preferential vaporization, i.e. fractionation (Koch et al., 2007; Koch and Gunther, 2007). This is true particularly in the case of metals, for which thermal relaxation time, i.e. the time it takes to transfer the pulse energy absorbed by free electrons to the lattice ions, takes place within a few hundred femtoseconds; therefore reduction of the laser pulse length to this time scale allows production of ultra-fine aerosol particles that more accurately reflect the bulk composition (Margetic et al., 2000; Gonzalez et al., 2004, 2005; Liu et al., 2004; Garcia et al., 2007; Perdian et al., 2008). As demonstrated here, fs-LA-ICP-MS analysis of the Singer gold

Table 1
Laser ablation and ICP-MS conditions

Laser	Hybrid system, 266 nm
Pulse length	~150 fs
Laser energy	0.1 mJ ± 2%
Spot size	20 μm
Energy density	320 TW cm^{-2}
Pulse rate	10 Hz
Ablation mode	Single spot
Ablation time	38 s
Carrier gas and flow rate	Ar 0.53 L/min; He 0.55 L/min
Dwell time	8 ms/AMU
Data acquisition mode	Time resolved (TRA)

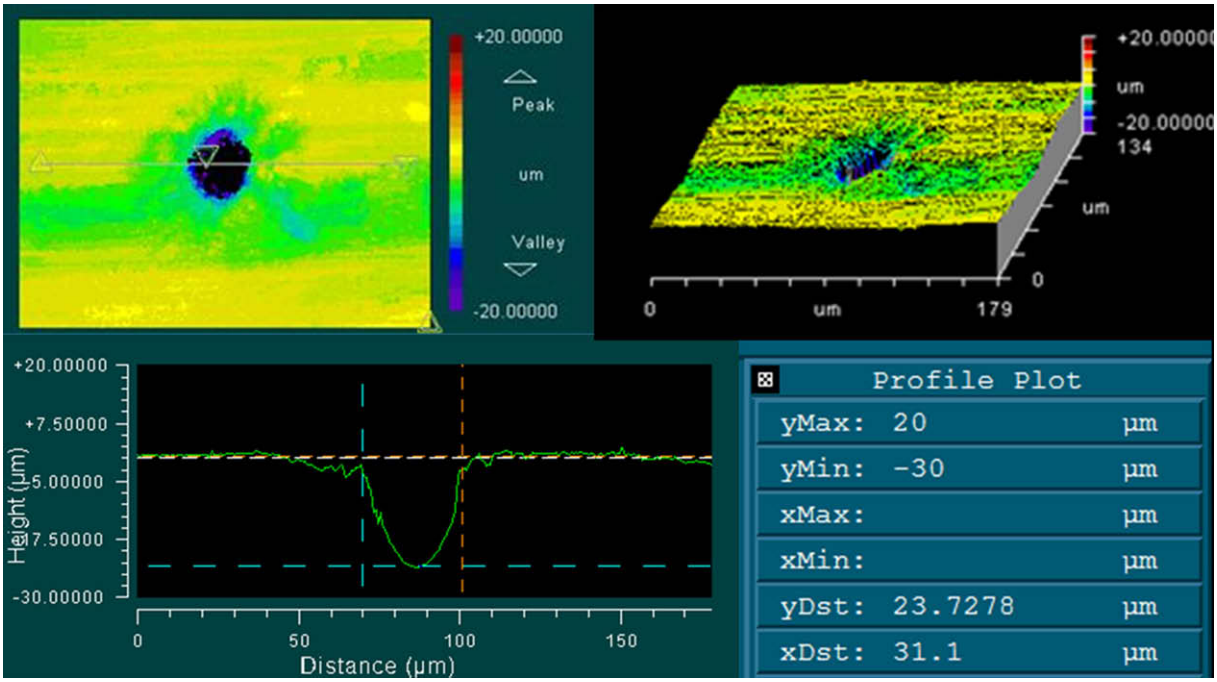

Fig. 4. White light interferometer microscope data and images and crater profile produced by femtosecond (~30 µm spot size) laser ablation on sample 4504-S.

fragments was successful in providing compelling support for the art historical and technical evidence, along with a better understanding of the relationship of the fragments to each other and to a previously unrelated object that appears similar by method of manufacture and decoration.

2. LA-ICP-MS methodology

Following an in-depth study of 23 samples from 22 gold fragments and objects at MCI using a 266-nm Nd:YAG ns-LA-ICP-MS system (Brostoff et al., 2007), samples were re-analyzed at Lawrence Berkeley National Laboratories (LBNL). The experimental system used at LBNL includes a fs-LA system consisting of a Spectra Physics Mai Tai Ti:sapphire seed laser and Spitfire regenerative amplifier. The 150-fs pulses at 800 nm are frequency tripled to obtain the 266-nm wavelength. The laser energy density is 320 TW cm^{-2}. An ICP-MS (VG PQ3 from VG Elemental) was used to analyze the ablated mass. In each analysis, the initial 10–15 s of ablation were discarded in order to allow for signal stabilization and removal of surface contaminants. Experimental details are provided in Table 1.

Nineteen isotopes were analyzed: ^{58}Ni, ^{60}Ni, ^{63}Cu, ^{65}Cu, ^{66}Zn, ^{68}Zn, ^{105}Pd, ^{106}Pd, ^{108}Pd, ^{110}Pd, ^{107}Ag, ^{109}Ag, ^{118}Sn, ^{120}Sn, ^{194}Pt, ^{195}Pt, ^{206}Pb, ^{208}Pb, and ^{237}AuAr^{+}. Introduction of a helium carrier gas was used to reduce signal spikes, the effect of which has been demonstrated in the literature (Gunther and Heinrich, 1999). Five 20 µm spots were analyzed on each sample. Select ablation craters and lines were examined with a Zygo New View 200 white light interferometer microscope in order to observe the physical effect of interaction of the gold foil with the femtosecond laser.

A set of gold standard reference materials (SRMs) was used for external, matrix-matched calibration. Major element calibration was accomplished for most samples using Royal Canadian Mint (RCM) gold alloy SRMs with silver in the range of 4–12% by weight, and copper in the range of 1–3% by weight (NIST 8068 and 8074). For trace element calibration, we used high purity gold RCM SRMs doped with 16 trace elements ranging from 5 to 119 ppm (NIST 8053, 8059, 8062, 8065). Data for major element calibration was not available for samples 4504 M, I, D, P, H, and G; therefore values for silver were extrapolated from trace element calibration up to about 50 ppm, and values for copper were extrapolated from trace element calibration up to about 100 ppm in these cases.

Analyte concentrations were calculated using linear response coefficients determined from the average integrated signal intensity in the SRMs after background correction and internal standardization to the gold argide ion (AuAr^{+}). Pd/Pt ratios were measured and calibrated directly, without reference to AuAr^{+}; this resulted in slightly greater precision over ratios taken from individually calculated concentrations for Pd and Pt derived from internal standardization. The limit of detection (LOD) for each isotope was determined as the concentration equivalent to three standard deviations (SD) above the background signal; these are shown in Table 3.

3. Results and discussion

3.1. Femtosecond laser ablation characteristics

White light interferometry examination of the samples after ablation revealed that fs ablation craters formed on the SRMs and samples had excellent characteristics. For example, as shown in the composite interferometer images of an ablation crater made on a gold reference sample (Fig. 4), the crater is actually about 30 µm in diameter, has very clean edges, no measurable debris, and is quite regular in shape, with cylindrical walls to a depth of about 15 µm. These desirable results cannot be wholly attributed to the use of

Table 2
Average regression coefficients as determined from Gold SRMs

Isotope	R^2coefficient	Isotope	R^2 coefficient
R^{58}Ni	0.9900	R^{107}Ag	0.9817
R^{60}Ni	0.9905	R^{118}Sn	0.9910
R^{65}Cu	0.9541	R^{195}Pt	0.9997
R^{68}Zn	0.9888	R^{208}Pb	0.9934
R^{108}Pd	0.9994	^{108}Pd/^{195}Pt	0.9998

R, ratio to AuAr^{+}.

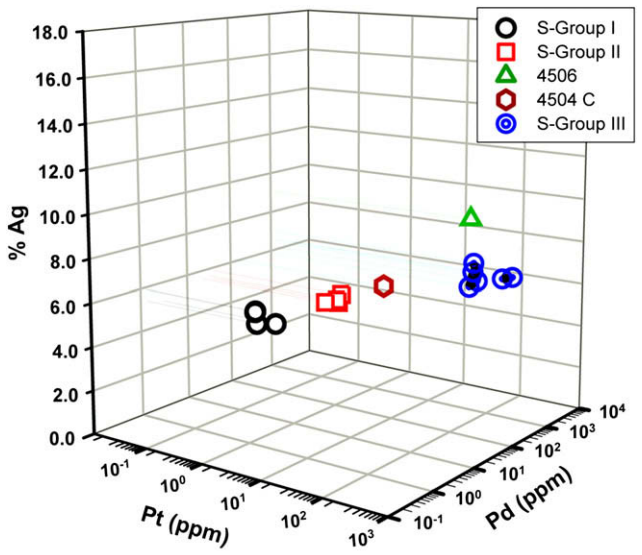

Fig. 5. Plot of Ag–Pd–Pt concentrations in Freer gold objects, as determined by femtosecond-laser ablation. Singer gold fragments: S-Group I (open circle), S-Group II (square), and S-Group III (filled circle); other gold object (upward triangle).

helium mixed into the carrier gas; rather, the ablation craters on the SRMs and samples visibly demonstrate that fs ablation of the ancient gold foil samples successfully avoids material redistribution, which is typically seen as visible melting, rough edges, and non-uniform craters from ablation with nanosecond lasers (Chichkov et al., 1996). As stated above, the superior physical characteristics of fs ablation may be attributed to significant reduction in thermal energy dissipation throughout the sample during the ablation process (Chichkov et al., 1996; Koch and Gunther, 2007). This evidence also points to even, repeatable ablation from spot to spot on the samples, and supports expectations that fs-LA should show high precision and reduced matrix effects, for which the external calibration to the gold standards cannot entirely compensate due to inevitable differences in chemistry and physical properties (Liu et al., 2004; Gonzalez et al., 2004, 2005; Koch and Gunther, 2007).

Three-point calibration curves obtained from the fine gold standards with fs-LA show excellent regression coefficients for most analytes over the various concentration ranges represented for different elements (Table 2). The regression coefficients illustrate that this analytical technique is excellent for the analysis of the gold reference samples. One exception here is the somewhat disappointing correlation coefficient of ^{65}Cu with fs-LA, for which there is no reliable explanation at this time; perhaps this arises from inhomogeneity in the standards relative to the spot size. Inhomogeneity in the samples also would be expected to have a more marked effect on the variation of relative standard deviation (RSD) from spot to spot, because of the small spot size used for femtosecond pulsed ablation.

3.2. Fingerprinting by fs-LA-ICP-MS

Ag, Pd and Pt concentrations in the samples obtained by fs-LA-ICP-MS are plotted in Fig. 5. The calculated concentrations are also provided in Table 3. Based on this analysis, three main groups of objects are readily distinguished. The clustering of points is also expressed by the low variation RSD, i.e. the variation of averaged values between ablation spots on the same sample, that exists for Pd/Pt concentration ratios in most cases, as shown in the bottom row of Table 3. This agreement allows confident identification, for example, in Group I of 4504 S with 4504 P, which were found to physically join together. On this basis, sample 4504 I may be grouped with 4504 S and P, whereas sample 4504 M is seen as distinct within Group I.

Table 3 also shows the calculated concentrations for Cu, Sn, Zn and Pb alongside those for Pd, Pt, and Ag. Results here are sorted first into Groups I-III by the directly measured Pd/Pt ratio, i.e. values obtained without normalization to $AuAr^+$. Sample results are then sorted within the respective groups by increasing Pd concentration, disclosing apparent subgroups (a-b) that correspond visually to the plot in Fig. 5. Finally, results are sorted from left to right within the designated subgroups by increasing Sn content. The LOD was approached for Ni in this analysis, most likely due to the small amount of ablated mass with the 20 μm spot size fs ablation; this element is therefore omitted from consideration. Relative standard deviations (RSD) for the average concentration variation between several spots on one sample (variation RSD) are shown. It should be noted that these values represent a combination of the instrumental technique and the heterogeneity of the sample.

In general, results in Table 3 confirm fairly consistent concentrations of silver, as well as copper and zinc, within experimental error, for the Singer fragments. The apparent heterogeneity of both copper and lead distribution in the samples is reflected in the higher variation RSD of these elements. Taken as a whole, however, the relatively high precision for multiple elements using fs-LA-ICP-

Table 3
Femtosecond LA-ICP-MS results with limits of detection (LOD)

	LOD (ppm)	Group Ia			Group Ib	Group IIa				Group IIb	Group IIIa					Group IIIb	
		4504 S	4504 P[a]	4504 I[a]	4504 M[a]	4504 A2	4504 A1	4504 O	4504 U	4504 C	4506	4504 L	4504 Q	4504 D[a]	4504 K	4504 H[a]	4504 G[a]
Ag107 (wt%)	1.26	5.9	5.3	5.9	5.1	5.6	5.7	5.9	5.5	6.1	9.0	7.0	6.1	5.8	6.6	6.2	6.2
% var (RSD)		4	14	5	27	7	6	3	8	6	3	5	11	8	5	7	5
Cu65 (wt%)	9.5	0.24	0.30	0.28	*0.12*	*0.43*	0.25	0.43	*0.30*	0.25	0.23	0.41	0.37	0.31	0.40	0.53	0.61
% var (RSD)		26	34	27	46	47	16	27	39	14	18	11	26	16	9	12	10
Sn118 (ppm)	0.25	348.32	369.54	402.48	312.70	362.52	376.93	534.32	609.01	418.85	380.54	811.37	858.92	966.76	1447.69	1089.45	1401.16
% var (RSD)		8	20	3	34	11	14	7	22	5	13	7	15	27	30	13	8
Pd108 (ppm)	0.03	1.29	1.35	*1.29*	2.84	22.58	32.21	38.69	35.61	123.01	1157.64	1176.32	1345.876	1089.26	1146.96	2409.68	3049.96
% var (RSD)		3	16	12	30	5	11	6	8	6	4	1	8	13	7	10	6
Pt195 (ppm)	0.05	1.09	1.11	1.08	*1.31*	2.01	2.52	2.62	2.46	6.38	45.86	52.06	55.53	46.13	51.55	104.21	133.74
% var (RSD)		2	9	7	16	2	11	4	4	6	6	2	9	9	3	9	3
Zn68 (ppm)	3.32	8.39	21.72	*7.87*	*14.22*	*10.16*	*25.45*	16.64	*18.37*	*11.20*	*16.46*	20.59	*15.04*	10.51	*12.48*	*10.85*	20.09
% var (RSD)		29	6	57	64	9	92	8	22	22	31	15	16	26	9	12	18
Pb 208 (ppm)	0.48	*146.64*	*737.92*	*358.72*	*84.56*	*290.79*	323.48	*1165.84*	*171.34*	*201.69*	178.84	*216.00*	*382.88*	*399.58*	*438.91*	156.90	*219.50*
% var (RSD)		46	86	81	58	58	33	65	45	19	34	43	56	49	14	24	49
Pd108/Pt195		**1.22**	**1.20**	**1.24**	**2.22**	**11.60**	**12.32**	***14.22***	***13.43***	**19.95**	**25.52**	**23.55**	**22.17**	**23.61**	**23.78**	**23.03**	**22.70**
% var (RSD)		**1**	**8**	**10**	**21**	**6**	**33**	**34**	**39**	**1**	**1**	**1**	**5**	**4**	**3**	**1**	**3**

var, variation; italics indicate greater uncertainly because of a combination of large RSD of measurement.
[a] Values for Ag and Cu extrapolated from calibration with fine gold SRMs.

MS allows refinement of the three major groups. Subgroups may correspond to individual gold plaque decorations made from the same sheet of gold, or to groups of related plaques. For example, within Group II, the two samples taken from 4504 A exhibit excellent matching precision. Results further suggest that while 4504 O and U have similar fingerprints to 4504 A, they probably originate from distinct objects. In Group III, samples 4504 L, Q and D are shown to be closely related. Of these, 4504 Q and D could be from the same dragon plaque, probably right facing, and do not seem to overlap according to the reconstructions.

The Group III profile links the majority of gold fragments and provides quantitative evidence for their origin in a single workshop. Groups I and II, which also contain fragments that are likely to have originated from dragon plaques, show general compositions and appearance consistent with manufacture from the Group III workshop; however, elemental results imply that the workshop either used multiple gold sources or a single source that is represented here by at least three distinct geochemistries (Leake et al., 1993). The fs-LA-ICP-MS analysis also helps to clarify some relationships. Sample 4504 C, which comes from a dragon plaque, appears closer to Group II than to Group III. Samples 4504 H and G are confirmed as distinct within Group III, although they do not match each other. One of the most interesting aspects of the results is the close alliance of sample 4506 with Group III; this sample comes from a stylistically related, gold-covered bronze disc (Fig. 2) that is otherwise not obviously related to the group of fragments, as mentioned above.

Overall, the results illustrate that trace element analysis can provide compelling evidence for establishing art historical relationships between the ancient Chinese gold objects by revealing compositionally and geologically related groups. LA-ICP-MS analysis of the fragments was expected to reveal either one Pd/Pt profile related to the gold source, as suggested in the literature (Watling et al., 1994; Guerra, 2004a), or none, due to random variation as a result of manufacture. Therefore, the emergence of three distinct Pd/Pt groupings is somewhat surprising. These results point out the value of using more than two elements to enable fingerprinting of the workshop manufacture of gold artifacts, especially given a relatively small sample set. Fs-LA-ICP-MS analysis, which has very good precision and greater freedom from matrix effects compared to conventional (nanosecond) laser ablation, leaves no doubt about the existence of compositional groupings. Ultimately, the careful use of LA-ICP-MS, which in this case involves application of a femtosecond laser, is shown to be capable of pinpointing fingerprints of single sheets of gold out of which an object was fashioned.

4. Conclusions

The study presented here was undertaken in order to shed light on provenance issues that were brought into focus by the technical study of a group of rare Chinese gold artifacts from the 5–6th century BCE in the collections of the Freer Gallery of Art and Arthur M. Sackler Gallery. A core group among the precious metal objects consists of an assortment of intricately worked gold fragments, which appear consistent in terms of method of manufacture, stylistic motifs and quality, overall elemental composition, and probably also archaeological origin, although they have been variously attributed to different archaeological sites. Two-thirds of the fragments have been proposed to belong to dragon-shaped ornamental plaques. Data generated from fs-LA-ICP-MS validate this analytical technique for quantitative analysis of major, minor and trace elements in minute gold samples, and underscore the importance of using more than one or two elements for 'fingerprinting' gold artifacts. Multi-element compositions based on the association of silver with trace palladium and platinum, and, to a lesser degree, tin, copper and zinc, allow us to establish patterns that support historical, technical and stylistic relationships, and enable matching of the fragments by origin of manufacture and even to one another with good precision.

Acknowledgments

The gold objects under study are part of the collection of the Freer Gallery of Art and Arthur M. Sackler Gallery, Smithsonian Institution. The gold foil fragments are part of The Dr Paul Singer Collection of Chinese Art of the Arthur M. Sackler Gallery, Smithsonian Institution; a joint gift of the Arthur M. Sackler Foundation, Paul Singer, the AMS Foundation for the Arts, Sciences, and Humanities, and the Children of Arthur M. Sackler, accession numbers RLS1997.48.4504 A-U. Work at LBNL was supported by the Office of Science, Office of Basic Energy Sciences, Chemical Sciences, Geosciences, and Biosciences Division, and the Deputy Administrator for Defense Nuclear Nonproliferation, Research and Development of the US Department of Energy under Contract No. DE-AC02-05CH11231. L.B. also wishes to thank Jeff Speakman for reviewing an earlier draft of this paper.

References

Brostoff, L.B., Gonzalez, J.J., Jett, P., Junchang, Y., Russo, R.E., 2007. In: Degrigny, C., van Langh, R., Joosten, I., Ankersmit, B. (Eds.), Proceedings of ICOM-CC Working Metal Group, Metal '07, Book I. Rijksmuseum, Amsterdam, pp. 30–37.
Chichkov, B.N., Momma, C., Nolte, S., von Alvensleben, F., Tunnermann, A., 1996. Applied Physics A Materials Science Processing 63 (2), 109–115.
Craddock, P.T., 1995. Early Metal Mining and Production. Smithsonian Institution Press, Washington, DC.
Garcia, C.C., Lindner, H., Niemax, K., 2007. Spectrochimica Acta, Part B: Atomic Spectroscopy 62, 13–19.
Gondonneau, A., Guerra, M.F., Barrandon, J.-N., 1996. Revue d'Archéométrie 20, 23–32.
Gonzalez, J., Liu, C.Y., Mao, X.L., Russo, R.E., 2004. Journal of Analytical Atomic Spectrometry 19, 1165–1168.
Gonzalez, J., Dundas, S.H., Liu, C., Mao, X.L., Russo, R.E., 2005. Journal of Analytical Atomic Spectrometry 21, 778–784.
Guerra, M.F., 2004a. Journal of Archaeological Science 31, 1199–1208.
Guerra, M.F., 2004b. Nuclear Instruments and Methods in Physics Research Section B 226, 185–198.
Guerra, M.F., 2004c. Journal of Archaeological Science 31, 1225–1236.
Guerra, M.F., Sarthre, C.-O., Gondonneau, A., Barrandon, J.-N.J., 1999. Archaeological Science 26 (8), 1101–1110.
Guerra, M.F., Calligaro, T., Radtke, M., Reiche, I., Riesemeier, H., 2005. Nuclear Instruments and Methods in Physics Research Section B 240 (1-2), 505–511.
Gunther, D., Hattendorf, B., 2005. Trends in Analytical Chemistry 24 (3), 255–265.
Gunther, D., Heinrich, C.A., 1999. Journal of Analytical Atomic Spectrometry 14, 1363–1368.
Hall, M.E., Brimmer, S.P., Li, F.-H., Yablonsky, L., 1998. Journal of Archaeological Science 25, 545–552.
Ixer, R.A., 1999. In: Young, S.M., Pollard, M., Budd, P., Ixer, R.A. (Eds.), Metals in Antiquity. BAR International Series 792, Oxford. Reprinted at http://www.rosiehardman.com/harvard.htm, 10 pp.
Jett, P., Brostoff, L., Dussubieux, L., 2007. In: Douglas, J., Jett, P., Winter, J. (Eds.), Scientific Research on the Sculptural Art of Asia: Proceedings of the Third Forbes Symposium at the Freer Gallery of Art. Archetype Publications in association with the Freer Gallery of Art, Smithsonian Institution, London, pp. 53–62.
Jones, M.P., 1983. In: Harvey, A.P., Kempe, D.R.C. (Eds.), The Petrology of Archaeological Artifacts. Clarendon Press, Oxford, pp. 330–350.
Koch, J., Gunther, D., 2007. Analytical and Bioanalytical Chemistry 387, 149–153.
Koch, J., Walle, M., Pisonero, J., Gunther, D., 2007. Journal of Analytical Atomic Spectrometry 21, 932–940.
Leake, R.C., Bland, D.J., Cooper, C., 1993. Transactions of the Institution of Mining and Metallurgy Section B: Applied Earth Science 102B, 65–82.
Liu, C., Mao, X.L., Mao, S.S., Zeng, X., Greif, R., Russo, R.E., 2004. Analytical Chemistry 76 (2), 379–383.
Margetic, V., Pakulev, A., Stockhaus, A., Bolshov, M., Niemax, K., Hergenröder, R., 2000. Spectrochimica Acta, Part B: Atomic Spectroscopy 55, 1771–1785.
Perdian, D.C., Bajic, S.J., Baldwin, D.P., Houk, R.S., 2008. Journal of Analytical Atomic Spectrometry 23, 325–335.
Ramage, A., Craddock, P., 2000. King Croesus' Gold. Harvard University Art Museums, Cambridge, MA.
Russo, R.E., Mao, X.L., Liu, H.C., Gonzalez, J., Mao, S.S., 2002. Talanta 57 (3), 425–451.
von Falkenhausen, L., 2006. Chinese Society in the Age of Confucius: (1000–250 BC). The Archaeological Evidence, Los Angeles, CA, p. 228.
Watling, R.J., Herbert, H.K., Deleve, D., Abell, I.D., 1994. Spectrochimica Acta 49B (2), 205–209.
Watling, R.J., Taylor, J.J., Shell, C.A., Chapman, R.J., Warner, R.B., Cahill, M., Leake, R.C., 1999. In: Young, S.M., Pollard, M., Budd, P., Ixer, R.A. (Eds.), Metals in Antiquity. BAR International Series, 792, Oxford, pp. 53–63.